A Phase I–II, Open-Label, Multicenter Trial to Determine the Dosimetry and Safety of ^{99m}Tc-Sestamibi in Pediatric Subjects

Sayena Azarbar*[1,2], Arash Salardini*[3], Nagib Dahdah[1], Joel Lazewatsky[4], Richard Sparks[5], Michael Portman[6], Paul D. Crane[4], Meng-Luen Lee[7], and Qi Zhu[4]

[1]Division of Pediatric Cardiology, CHU Ste-Justine, University of Montreal, Quebec, Canada; [2]Montreal Heart Institute, University of Montreal, Quebec, Canada; [3]Department of Neurology, Yale School of Medicine, New Haven, Connecticut; [4]Lantheus Medical Imaging, North Billerica, Massachusetts; [5]CDE Dosimetry Services, Knoxville, Tennessee; [6]Seattle Children's Research Institute, Seattle, Washington; and [7]Division of Pediatric Cardiology, Changhua Children's Christian Hospital, Changhua, Taiwan

Myocardial perfusion imaging has long been used off label by practitioners attending for children with cardiac aliments. To provide clinicians with evidence-based dosage recommendation, a phase I–II, open-label, nonrandomized, multicenter trial was therefore designed using ^{99m}Tc-sestamibi in pediatric subjects (registered under www.clinicaltrials.gov identifier no. NCT00162045). **Methods:** Safety and pharmacokinetic data were collected from 78 subjects using either a 1-d imaging protocol (3.7–7.4 MBq/kg, followed by 11.1 MBq/kg) or a 2-d protocol (7.4 MBq/kg for both rest and stress). Anterior and posterior planar images were collected at 15 min, 1.5 h, 4 h, and 8 h. Blood and urine samples were collected at predetermined times. **Results:** Subjects included 39 children (mean age ± SD, 8.5 ± 2.04 y) and 39 adolescents (mean age ± SD, 13.6 ± 1.39 y). Mean estimated organ-absorbed doses to the upper large intestine, small intestine, gallbladder wall, and lower large intestines were 0.082, 0.043, 0.042, and 0.035 mSv/MBq, respectively. All patients tolerated the radiotracer without serious adverse effects. Significant differences were observed in the liver, upper large intestine contents, and small intestine contents between rest and stress imaging. The effective dose equivalent and effective dose averages were lower in adolescents than younger children (0.011 and 0.019 mSv/MBq, respectively; $P <$ 0.0001). Percentage injected doses (%IDs) corrected for radioactive decay in all dosimetry-evaluable subjects at 15 min and 4 h were 1.9% and 1.2% in the myocardium. Similarly in the lungs, the %ID for all dosimetry-evaluable subjects was 4.9% at 15 min after injection. At rest, the %ID in the liver decreased from a maximum of about 26% at 15 min to less than 9% at 90 min. With stress, values decreased from 15% to 7%, respectively. **Conclusion:** The estimates of radiation dosimetry, pharmacokinetic parameters, and safety profile in this study population are similar to published studies based on body-mass extrapolations from studies in adults. As such, applying current ^{99m}Tc-sestamibi dosing regimens for 1- and 2-d protocols based on those extrapolations will result in the expected radiation dose in children and adolescents.

Key Words: myocardial nuclear imaging; safety; pharmacokinetics; children

J Nucl Med 2015; 56:728–736
DOI: 10.2967/jnumed.114.146795

Received Oct. 14, 2014; revision accepted Mar. 19, 2015.
For correspondence or reprints contact: Nagib Dahdah, 3175 Côte Ste-Catherine, CHU Ste-Justine, Division of Pediatric Cardiology, Montreal, Qc, H3T 1C5, Canada.
E-mail: nagib.dahdah.hsj@ssss.gouv.qc.ca
*Contributed equally to this work.
Published online Apr. 9, 2015.

The role of myocardial perfusion imaging for the assessment of risk and viability of ischemic myocardium is well established in the adult population. Among the radiotracers used, ^{99m}Tc-sestamibi (Cardiolite; Lantheus Medical Imaging) has shown superior characteristics as a tracer for myocardial perfusion imaging with SPECT. The role of this tracer is less established in the pediatric population because of the relatively smaller sample sizes and lack of data regarding dosing (*1*). Myocardial perfusion imaging is used in children primarily to identify coronary perfusion abnormalities such as occur in Kawasaki disease, anomalous left coronary artery from pulmonary artery, and transposition of the great arteries among other conditions (*2*,*3*).

All radiopharmaceuticals subject patients to modest doses of radiation, which is of special significance in children, in whom early exposure to radiation may disproportionately increase the risk of neoplastic disease in later life. Several studies have assessed the radiation exposure due to ^{99m}Tc-sestamibi in the adult populations (*4*), and others have estimated the corresponding figures for children using mathematic modeling (*5*,*6*). However, to date no studies of estimates of radiation dose in children have been published. Consequently, there is little systematic data on general safety and pharmacokinetics of ^{99m}Tc-sestamibi in this population.

In this study, we present the results of a phase I–II open-label, multicenter trial conducted with the aim of determining dosimetry, pharmacokinetics, and safety of ^{99m}Tc-sestamibi when used at rest or stress in 2 age groups of children (ages, 4–11 and 12–16 y).

MATERIALS AND METHODS

The primary endpoint of the study was to determine the absorbed dose of ^{99m}Tc-sestamibi, at rest or stress, in the 2 subject groups: children and adolescents. The secondary aims were to determine the biodistribution and safety in the same setup.

Patient Selection and Ethics

The study was performed at 12 sites in the United States, Canada, and Taiwan. On the basis of previous dosimetry trial experience in adults, a sample size of at least 24 subjects was considered adequate for the assessment of dosimetry with ^{99m}Tc-sestamibi in pediatric subjects. A sample size of at least 24 subjects was also considered adequate for the assessment of the kinetics of ^{99m}Tc radioactivity (referred to hereafter as pharmacokinetics) after administration of ^{99m}Tc-sestamibi in pediatric subjects. The subjects chosen were between the ages of 4 and 16 y. Assent from the children in addition to written consent from

the subject's legal guardians was obtained. All subjects were able to participate in the imaging procedure and had no physical barriers to doing so. We excluded wards of the state or institutionalized children and those with significant laboratory abnormalities including creatinine greater than 2.5 mg/dL, liver enzyme greater than 2 times the upper limit of normal, or platelet count less than 100,000/mm^3. We also excluded pregnant subjects and those with history of the following: illicit drug or alcohol abuse within 6 mo of the enrollment, life expectancy of less than 6 mo, having received investigation products or devices within 30 d of enrollment, allergy to ^{99m}Tc-sestamibi, and having received radiopharmaceuticals for which the time since injection was equal to or less than 10 times the physical half-life of the radiopharmaceutical.

Because of methodologic issues as described below in the "Pharmacokinetics" section, more patients were enrolled than originally planned.

Subjects were considered part of one or more populations for analysis purposes: DE (dosimetry-evaluable: all subjects who completed the imaging protocol), PE (pharmacokinetics-evaluable: those for whom the analysis of blood radioactivity was performed after the correction and standardization of procedures described later), PN (pharmacokinetics-nonevaluable: those in the DE population who did not fulfill the PE criteria), and SA (safety-evaluable: subjects who received at least 1 injection of ^{99m}Tc-sestamibi). Any enrolled subject not part of at least one of the first two or the last of these was unevaluable.

The subjects chosen had been previously scheduled for clinically indicated scans. There was a small increase (about 1% of the effective dose [ED] assuming a total dose of 925 MBq) in exposure due to the transmission portion of the acquisition for those patients in the DE population. The guidelines used included the Declaration of Helsinki, the International Conference on Harmonization, Good Clinical Practices, and the Food and Drug Administration regulations (21 Code of Federal Regulations Parts 50 and 56) for the protection of the rights and welfare of human subjects participating in biomedical research. It was approved by the institutional review boards of all enrolling sites. Finally, this study was registered under www.clinicaltrials.gov, identifier number NCT00162045.

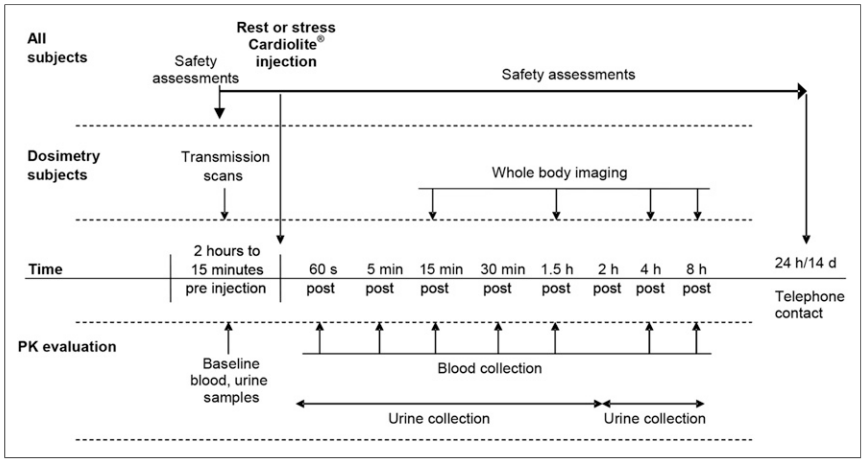

FIGURE 1. Graphical representation of overall study design. Safety was assessed by monitoring vital signs, physical examination, electrocardiograms, clinical laboratory tests, and adverse events. In addition, subject's parent or legal guardian was contacted by telephone or visited within the hospital at 24 ± 12 h and again at 14 d after completion of rest or stress study for safety evaluations. Dosimetry was assessed by acquiring series of whole-body images at time points specified above. Pharmacokinetics were assessed by collection of blood and urine samples at time points specified above. PK = pharmacokinetics.

Study Design

We used ^{99m}Tc-sestamibi (Kit for the Preparation of Technetium Tc99m Sestamibi for Injection). ^{99m}Tc-sestamibi was reconstituted with sterile, nonpyrogenic, oxidant-free sodium pertechnetate ^{99m}Tc injection. The pH of the reconstituted product was 5.5 (5.0–6.0). No bacteriostatic preservative was present. The precise structure of the technetium complex is ^{99m}Tc [MIBI]6+, where MIBI was 2-methoxyisobutyl isonitrile. ^{99m}Tc decays by isomeric transition with a physical half-life of 6.02 h (*7*).

The study was designed as a phase I–II open-label, nonrandomized, multicenter study in pediatric subjects undergoing SPECT scanning with ^{99m}Tc-sestamibi at rest or stress (Fig. 1). Dosimetry and pharmacokinetic assessments were performed in parallel with the imaging procedures, and patients were monitored for safety and adverse events for 24 ± 12 h and for 14 d for serious adverse events via the phone (Fig. 1). Twelve centers were initiated, and 10 (5 in the United States, 2 in Canada, and 3 in Taiwan) of these enrolled subjects. The study was conducted between January 28, 2005, and June 15, 2007 (29 mo). The study sponsor, Bristol-Myers Squibb Medical Imaging, Inc. (BMSMI, now Lantheus Medical Imaging) monitored the study. Clinical supplies were also the responsibility of BMSMI or its designee. Analysis of the whole-body data was performed on all subjects with whole-body images by CDE Dosimetry Services, Inc. The clinical database was managed by ICON Clinical Research, Ltd. Bristol-Myers Squibb Research and Development conducted the blood pharmacokinetic parameter analysis. BMSMI was responsible for the statistical analyses. The final, hard-locked database was maintained by BMSMI.

Dose Selection and Imaging

The dose of ^{99m}Tc-sestamibi was chosen to be the lowest possible dose that would permit accurate pharmacokinetic and dosimetric determinations while providing adequate SPECT imaging. On the basis of previously published data (*5,8–10*), this was determined to be 3.7–11.1 MBq/kg (0.1–0.3 mCi/kg). The source of the sestamibi was the commercially available ^{99m}Tc-sestamibi. Two protocols were used: 1 institution used a 2-d SPECT imaging protocol for which 7.4 MBq/kg (0.2 mCi/kg) was used both at rest and stress. The other institutions used 1-d SPECT imaging protocols, administering 3.7–7.4 MBq/kg (0.1–0.2 mCi/kg) at rest or stress for the first imaging procedure, followed by 11.1 MBq/kg (0.3 mCi/kg) at rest or stress for the second SPECT imaging procedure. Results from all institutions were used in the analysis.

All doses were assayed before administration. In addition, the syringe containing the dose was assayed after administration and the net injected dose calculated, corrected for radioactive decay to the time of dosing.

The design of the imaging protocol was consistent with the methods recommended in MIRD pamphlet 16 (*11*). All images were part of either a 1- or 2-d rest–stress study performed for the patient's medical care. Study-related imaging for a given patient was performed during either the rest or the stress portion of the study (but not both) using whole-body scanning, a high-resolution low-energy collimator, and a matrix of 256 × 1,024 as appropriate with a speed of between 8 and 15 cm/min. Acceptable γ camera quality control was required before the acquisition of all image data. All images were corrected for uniformity and linearity. Transmission and reference whole-body scans (with and without the patient in place,

respectively, and both before injection of the patient) were obtained using 1 head of a dual-head γ camera before dose administration with an external ^{57}Co flood source or a ^{99m}Tc-filled flood source.

After ^{99m}Tc-sestamibi administration, anterior and posterior whole-body images were acquired simultaneously with the same 2-head γ camera (in the 180° opposed configuration) with the patient supine at nominal times of 15 min, 1 h, 4 h, and 8 h after dose administration. A small calibrated reference source (0.74–1.48 MBq [20–40 μCi] of ^{99m}Tc) was prepared with radioactivity assayed on the same dose calibrator at the site used for dose assay. This source was included within the camera field of view but outside the patient's body outline (typically next to the head) in each anterior–posterior whole-body scan.

Blood and Urine Sampling

Blood samples were collected in heparinized tubes (3 mL) before injection and at 1, 5, 15, and 30 min as well as 1.5, 4, and 8 h after injection. Duplicate aliquots were used for each sample. Baseline urine samples were collected between 15 min and 2 h before the injection. All urine up to 8 h after the injection was collected. Total volume for each collection was measured and 2 aliquots obtained from each for ^{18}F assay.

Dosimetry and Pharmacokinetic Analysis

Radiation dosimetry analysis was conducted by the dosimetry core laboratory, CDE Dosimetry Services, Inc., from image data provided by the participating sites. Absorbed radiation dose to the salivary glands, total body, and standard organs (included in the age-appropriate MIRD (*11*) pediatric phantoms (*12*)) were estimated. Organ retention was obtained for all organs using regions of interest drawn around the whole body as well as each of the visibly appreciable source organs. The whole body was segmented into subregions of equal anterior–posterior thickness to allow appropriate whole-body attenuation correction. Organ radioactivity values were obtained by geometric mean of corresponding regions corrected for attenuation and for activity contained within underlying and overlying tissues. Values of the fractional injected radioactivity in each organ were determined using the region-specific attenuation-corrected whole-body counts value from the first image. Fractional injected doses per organ were subjected to multiterm nonlinear regression using exponential functions and the results integrated to obtain organ residence times. Radiation doses were calculated from these data using OLINDA/EXM, version 1.0.

Absorbed doses were reported in both mSv/MBq and rem/mCi for each organ. Estimations of the effective dose equivalent (EDE) and ED (both tissue-weighted measures of stochastic risk due to radiation exposure) were determined in both mSv/MBq and rem/mCi using the methodology described in International Commission on Radiological Protection (ICRP) publication 26 (*13*) and ICRP publication 60 (*14*), respectively. Descriptive statistics were calculated for organ retention by nominal time, for residence times, and for dosimetry parameters using the DE population. This was done as well for each analysis group (rest children, rest adolescents, stress children, stress adolescents), for combinations of these groups (children, adolescents, rest, and stress), and for the overall DE population. The percentage injected dose (%ID) per mL in blood samples was calculated by comparison with the ^{99m}Tc-pertechnetate standards, and estimated whole-body volume was calculated assuming 70 mL of blood per kg of whole-body weight.

The primary pharmacokinetic endpoints were expressed in terms of the %ID. Blood radioactivity was determined by radiometric γ well counter assay, and %ID per estimated whole-body blood volume (WBBV) was calculated. After the initial enrollment (31 subjects enrolled from January 2005 through September 2006), the pharmacokinetic data were examined. After initial analysis, some inconsistency in the pharmacokinetic standards was found due to the use of ^{99m}Tc-sestamibi to prepare the standards combined with human error in performing assay dilutions and pipetting. The former was due to the tendency of ^{99m}Tc-sestamibi to adhere to syringes and vessels during dilution. We therefore substituted ^{99m}Tc-pertechnetate for ^{99m}Tc-sestamibi for creation of the counting standards, validated the integrity of the dilution procedure, and then revised the protocol and enrolled additional subjects. Before reinitiation of enrollment, well counters at each of the sites were subjected to prespecified operational qualification. Additionally, onsite guidance and staff training was provided during initial and subsequent sample processing and γ-counter analysis of pharmacokinetic specimens as necessary. Subsequently, 48 additional subjects were enrolled from March to May 2007, providing a total of 79 subjects. The ^{99m}Tc-pertechnetate standard was used in 47 of the 48 additional subjects. The remaining enrolled subject was deemed not to be evaluable for pharmacokinetics and was excluded from the analysis as were the earlier subjects for whom the standard was prepared using ^{99m}Tc-sestamibi or for whom the blood sample assay was performed incorrectly.

The radioactivity (in %ID) in blood over time (in h) was plotted and the areas under the curve determined for each patient (using trapezoidal and log-trapezoidal methods) between time zero and the last radioactivity time point (AUC(0-T) [%ID h]). The curve was extrapolated from zero to infinite time (AUC(INF) [%ID h]) and the terminal elimination (T1/2 [h]) and mean residence time (MRT [h]) determined. Radioactivity (%ID) in urine after ^{99m}Tc-sestamibi administration was also determined. The slope of the terminal phase of the blood %ID–time profile was determined with the weighting factor of 1 by the methods of least squares. T1/2 was estimated as ln2/(slope of the terminal phase). MRT was calculated using the ratio of area under the moment curve divided by the area under the curve.

Pharmacokinetic parameters were estimated with validated noncompartmental analysis software (Kinetica, as part of Thermo Fisher Scientific's eToolbox, version 2.6.1; Thermo Fisher Scientific). The estimated pharmacokinetic parameters in blood were summarized in 2 groups: the PE population and separately in those who were in both DE and PE populations. Pharmacokinetic parameters were not summarized in subjects who were not evaluable for pharmacokinetics (PN). Individual pharmacokinetic profiles of %ID in estimated WBBV were provided using %ID versus time plots. The %ID in urine from 0 to 2 and 2 to 8 h after injection was summarized at each time point for all subjects by PE and PN populations. Listings of %ID in urine for all subjects were provided. However, urine pharmacokinetic parameter estimation and pharmacokinetic profiling were not conducted.

ANOVA-based models were run to determine the significance of rest–stress and child–adolescent effects in dosimetry and pharmacokinetic endpoint results, and further tests of multiple comparison were conducted using the Duncan multiple-range test at 5% comparisonwise type I error between these analysis groups. These tests of comparison were post hoc. This study was not powered to test any a priori hypothesis of clinically relevant differences, and the results of comparisons do not provide any statistical claims.

Safety assessments included adverse events (AEs, up to 24 ± 12 h after injection of ^{99m}Tc-sestamibi), serious adverse events (SAEs, up to 14 d after completion of the rest or stress whole-body imaging study), vital signs (systolic and diastolic blood pressure and heart rate), electrocardiograms, laboratory values (hematology, chemistry, and urinalysis), and limited physical examinations.

Statistical Methods

All statistical work was done using SAS software, version 8.02. Within each analysis population (DE, PE, PN, and SA) results were determined for each of the 4 analysis subgroups: children (age, 4–11 y), rest study; children (age, 4–11 y), stress study; adolescents (age, 12–16 y), rest study; adolescents (age, 12–16 y), stress study.

Descriptive statistics (*n*, mean, median, SD, minimum, and maximum) were calculated for all parameters derived from the whole-body

TABLE 1
Demographics of Study Population

Characteristic	Children	Adolescents	Total
Mean age ± SD (y)			
All	8.5 ± 2.04 (39)	13.6 ± 1.39 (39)	11.1 ± 3.10 (78)
Rest subjects	8.6 ± 2.18 (21)	13.5 ± 1.37 (22)	11.1 ± 3.07 (43)
Stress subjects	8.5 ± 1.92 (18)	13.8 ± 1.42 (17)	11.1 ± 3.18 (35)
Mean height ± SD (cm)			
All	135.4 ± 14.68 (39)	162.3 ± 11.12 (39)	148.8 ± 18.70 (78)
Rest subjects	136.3 ± 12.65 (21)	162.0 ± 11.61 (22)	149.5 ± 17.68 (43)
Stress subjects	134.4 ± 17.07 (18)	162.5 ± 10.79 (17)	148.1 ± 20.10 (35)
Mean weight ± SD (kg)			
All	34.5 ± 11.80 (39)	60.8 ± 18.40 (39)	47.7 ± 20.26 (78)
Rest subjects	35.1 ± 11.78 (21)	61.4 ± 18.97 (22)	48.6 ± 20.57 (43)
Stress subjects	33.9 ± 12.13 (18)	60.0 ± 18.18 (17)	46.6 ± 20.11 (35)
Sex (male/female)			
All	26/13	26/13	52/26
Rest subjects	14/7	13/9	27/16
Stress subjects	12/6	13/4	25/10
Race (all)	39	39	78
White	16	15	31
Black	1	5	6
Asian	20	15	35
Other	2	4	6
Rest studies	21	22	43
White	9	11	20
Black	0	1	1
Asian	10	8	18
Other	2	2	4
Stress studies	18	17	35
White	7	4	11
Black	1	4	5
Asian	10	7	17
Other	0	2	2

Data in parentheses are *n*.

images in the course of the dosimetry analysis as well as pharmacokinetic parameters. ANOVA-based models were run on organ radioactivity, residence time, and radiation dose estimates for organs of importance in dosimetry and pharmacokinetic endpoints. The study was not powered to conduct intergroup comparisons in dosimetry or pharmacokinetic results, as these comparisons are considered exploratory and post hoc.

Descriptive statistics (*n*, mean, median, SD, minimum, and maximum) were calculated for all quantitative safety parameters. Frequencies and percentages were determined for all qualitative safety parameters. All summaries were based on the SA population, and AEs were coded using the MedDRA dictionary.

RESULTS

Demographics

Seventy-eight patients were used in the overall analysis, among whom the median age was 11.5 y (range, 4–16 y). Of these, 39 subjects were aged 4–11 (children), and 39 fell within the 12–16 age range (adolescents). Two thirds of the patients were male, which roughly corresponds to the sex distribution of the conditions for which the SPECT imaging is indicated (*15,16*). Forty-five percent of subjects in the study self-identified (or were identified by legal guardians) as Asian and 40% as White, which is consistent with the expectations based on the disease indication and sites of recruitment (Table 1).

Among the 31 subjects enrolled before the problems with the blood sampling and analysis were identified, none were PE and 28 were DE (one for failure to inject due to inability to gain intravenous access; another due to dose infiltration at the injection site; and a third, for failure to acquire the necessary images). Of the 48 additional subjects, 18 were both DE and PE, 1 was DE but not PE due to other problems with the pharmacokinetic standard, 28 were PE and not DE as dosimetry images were not required for this

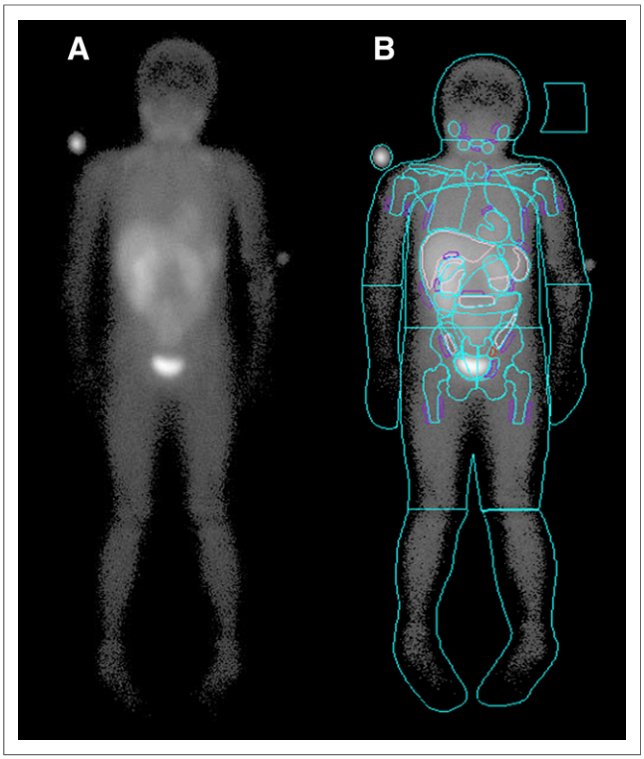

FIGURE 2. Example of dosimetry image from first whole-body emission imaging of subject 002-005, a 6-y-old female, shown using logarithmic intensity scale without regions (A) and with regions (B). Image data on both left and right are derived by taking geometric mean, pixel by pixel, of anterior image and mirrored posterior image, both from first time point. It is shown only for purposes of visual representation of subject and organs with significant activity using both anterior and posterior data. It was not used in this form for any calculations. Small amount of radioactivity seen adjacent to subject's left arm may be spot of contamination after injection of compound.

second cohort, and finally 1 was neither PE nor DE nor SA due to withdrawal of the subject before dosing. The subject who was neither PE nor DE nor SA is therefore not among the subjects evaluated. Overall, 18 subjects were both DE and PE, 29 were DE but not PE, 28 were PE but not DE, 3 were evaluable only for safety, and 1 was nonevaluable.

Dosimetry

For the 47 DE subjects, the largest mean estimated organ-absorbed dose was to the upper large intestine (ULI) wall at 0.082 mSv/MBq (0.30 rem/mCi). The next largest absorbed doses in decreasing order were to the small intestine (SI) wall at 0.043 mSv/MBq (0.16 rem/mCi), the gallbladder wall at 0.042 mSv/MBq (0.16 rem/mCi), and the lower large intestine wall at 0.035 mSv/MBq (0.13 rem/mCi). Significant differences were observed in liver, ULI contents, and SI contents between rest and stress subjects (liver, $P = 0.026$; ULI, $P = 0.015$; SI, $P = 0.0002$) and between children and adolescents (liver, $P < 0.0001$; ULI, $P = 0.0016$; SI, $P < 0.0001$) (Fig. 2).

The average EDE for ^{99m}Tc-sestamibi was 0.019 mSv/MBq (0.072 rem/mCi). The average ED for ^{99m}Tc-sestamibi was 0.015 mSv/MBq (0.055 rem/mCi). Mean ED was significantly higher in children than in adolescents ($P < 0.0001$). Similarly, mean EDE was significantly higher in children than in adolescents ($P < 0.0001$) (Table 2).

The rest–stress effect was significant in the models of residence time in the liver ($P = 0.0025$), SI contents ($P = 0.0015$), and ULI ($P = 0.002$). This effect was consistent with the visual observations of shifts of radioactivity between rest and stress studies in the organs of the hepatobiliary pathway. For %ID corrected for radioactive decay, myocardial %ID reached a value of approximately 1.5%–2% at 15 min after injection, decreasing to about 1.2% at 4 h. In the lungs, the %ID was low, with a maximum of approximately 4.9% at 15 min after injection. Similar %ID values in the myocardium and lung were obtained between all analysis groups. Liver %ID was similar in both children and adolescents, but significant differences ($P < 0.0001$) were observed between rest and stress. In rest subjects, the %ID in the liver decreased rapidly from a maximum of approximately 26% at 15 min to less than 9% at 90 min. With stress, values decreased from 15% at 15 min to 7% at 90 min. Significant differences between rest and stress of a similar magnitude were also observed ($P = 0.0002$) in the SI contents (Figs. 3 and 4).

TABLE 2
Absorbed Dose Estimates for All DE Subjects in mSv/MBq

Organ	Mean	SD	Minimum	Maximum
Adrenals	0.0074	0.0021	0.0048	0.012
Brain	0.0024	0.0011	0.00080	0.0053
Breasts	0.0027	0.0010	0.0012	0.0054
Gallbladder wall	0.042	0.031	0.011	0.19
Lower large intestine wall	0.035	0.020	0.013	0.14
SI wall	0.043	0.023	0.013	0.11
Stomach wall	0.0087	0.0028	0.0053	0.016
ULI wall	0.082	0.046	0.019	0.24
Heart wall	0.010	0.0034	0.0057	0.021
Kidneys	0.023	0.0067	0.012	0.037
Liver	0.014	0.0053	0.0073	0.030
Lungs	0.0085	0.0026	0.0051	0.016
Muscle	0.0048	0.0014	0.0032	0.0084
Ovaries	0.018	0.0061	0.0093	0.037
Pancreas	0.0090	0.0029	0.0054	0.016
Red marrow	0.0076	0.0038	0.0039	0.022
Bone surfaces	0.011	0.0033	0.0068	0.020
Salivary glands	0.0057	0.0031	0.0014	0.014
Skin	0.0024	0.00088	0.0013	0.0049
Spleen	0.012	0.0043	0.0049	0.024
Testes	0.0040	0.0015	0.0018	0.0075
Thymus	0.0035	0.0013	0.0016	0.0068
Thyroid	0.0070	0.0038	0.0025	0.024
Urinary bladder wall	0.027	0.012	0.010	0.060
Uterus	0.015	0.0055	0.0079	0.030
Total body	0.0061	0.0018	0.0041	0.011
ED	0.015	0.0060	0.0076	0.042
EDE	0.019	0.0078	0.0088	0.050

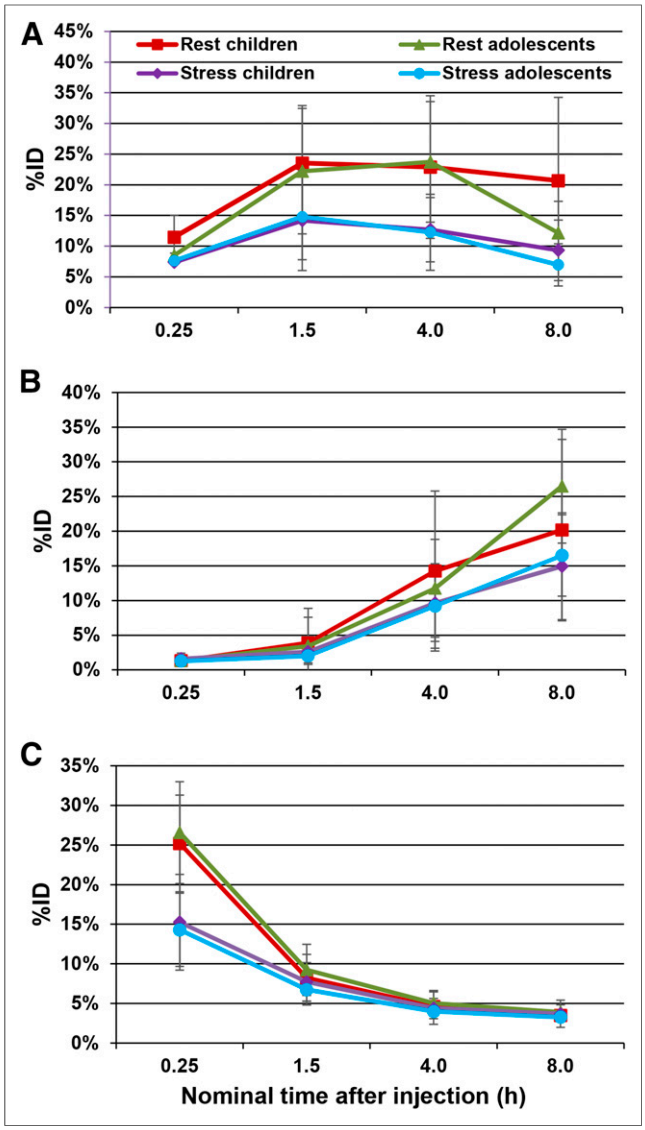

FIGURE 3. Whole-organ radioactivity as function of time in whole body (A), heart wall (B), and lungs (C).

The effects of all of these factors may be observed in Supplemental Appendices 1 and 2 (supplemental materials are available at http://jnm.snmjournals.org), in which the individual organ dosimetry as well as both the ED and the EDE have been broken out by stress versus rest and children versus adolescents.

Pharmacokinetics

For the 46 PE subjects in this study, the radioactivity after ^{99m}Tc-sestamibi administration had similar blood pharmacokinetic profiles in children and adolescents, whereas the profiles were significantly different between rest and stress subjects ($P = 0.0013$). The mean %ID in WBBV was 53.5% at 1 min in stress subjects, followed by a rapid decline to 5.1% at 5 min, compared with that of 28.4% at 1 min and 5.4% at 5 min in rest subjects. A similar trend was observed in 18 subjects in the DE + PE population.

The mean ± SD of the blood pharmacokinetic parameters for the PE population, AUC(0-T), AUC(INF), terminal elimination T1/2, and MRT, are summarized in Table 3 for the 4 analysis groups.

The overall pharmacokinetic parameters (Table 4) for radioactivity in blood after ^{99m}Tc-sestamibi administration were an AUC (0-T) of 5.09 ± 1.76 %ID·h, AUC(INF) of 6.59 ± 2.59 %ID·h, terminal elimination T1/2 of 3.45 ± 1.13 h, and MRT of 3.62 ± 1.27 h. Higher AUC values were observed in stress subjects (AUC (0-T), $P = 0.019$; AUC(INF), $P = 0.04$) and in children (AUC(0-T), $P = 0.0497$; AUC(INF): $P = 0.026$), with differences that were statistically significant. No significant differences were observed in terminal elimination T1/2 and MRT values. The overall mean urinary excretion of radioactivity by 6 h was 13.8% ± 8.59%, with the majority recovered during the first 2 h after ^{99m}Tc-sestamibi administration. Urine excretion rates are included in Table 4.

Safety Results

The overall incidence of AEs was 19%, and the incidence was higher in children (28%) than in adolescents (10%). One child experienced an SAE (asthma), and 1 child discontinued due to an

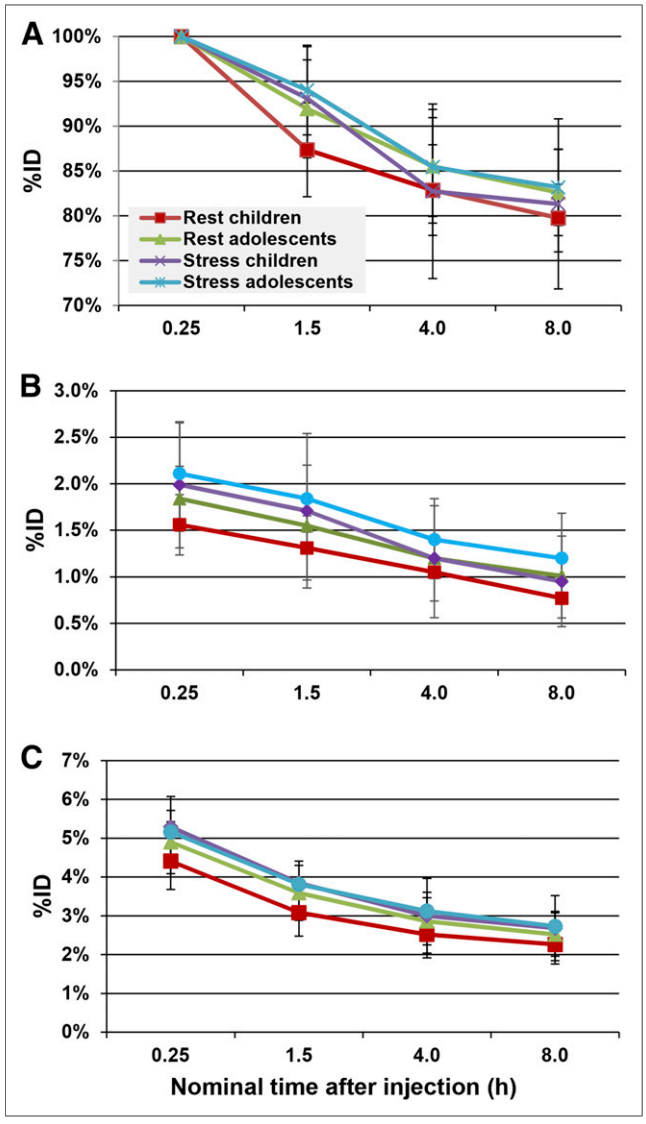

FIGURE 4. Whole-organ radioactivity as function of time in small bowel (A), ULI (B), and liver (C).

TABLE 3
Pharmacokinetic Measures (%ID in Estimated WBBV) in Blood by Time Point (PE Population)

Analysis group	1 min	5 min	15 min	30 min	1.5 h	4 h	8 h
Rest subjects							
Children	38.6 ± 20.57	4.5 ± 1.46	1.7 ± 0.79	1.2 ± 0.45	0.7 ± 0.26	0.4 ± 0.18	0.3 ± 0.15
Adolescents	19.0 ± 21.78	6.2 ± 3.11	1.5 ± 0.55	1.0 ± 0.45	0.6 ± 0.22	0.3 ± 0.09	0.2 ± 0.07
All	28.4 ± 23.05	5.4 ± 2.62	1.6 ± 0.67	1.1 ± 046	0.6 ± 0.25	0.4 ± 0.14	0.3 ± 0.12
Stress							
Children	52.8 ± 17.31	4.9 ± 1.46	2.1 ± 0.81	1.4 ± 0.54	0.8 ± 0.26	0.4 ± 0.16	0.3 ± 0.16
Adolescents	54.3 ± 22.08	5.4 ± 1.81	2.0 ± 0.34	1.3 ± 0.21	0.7 ± 0.14	0.3 ± 0.12	0.3 ± 0.10
All	53.5 ± 22.11	5.1 ± 1.60	2.0 ± 0.62	1.4 ± 0.42	0.7 ± 0.21	0.4 ± 0.15	0.3 ± 0.14
Total	38.8 ± 24.68	5.3 ± 2.20	1.8 ± 0.67	1.2 ± 0.45	0.7 ± 0.23	0.4 ± 0.14	0.3 ± 0.13

Data units are mean ± SD.

AE (infusion site reaction). Both events were considered unlikely related to the study drug by the investigators (Table 5).

One adolescent had laboratory values that were considered clinically significant (hematology values 8 ± 2 h after injection), and none of the subjects had positive urine values that were considered clinically significant. Mean changes from baseline in vital signs and electrocardiograms were not clinically significant. Few physical examination result changes were observed.

DISCUSSION

The study was developed in collaboration with the Food and Drug Administration, with a planned enrollment of 24 subjects. However, technical issues with the preparation of the pharmacokinetic standard and with on-site γ-counter analysis led to an increase in enrollment to 79 subjects (with 78 subjects dosed). Of these, image acquisition and quantification for dosimetry estimates were conducted in 47 subjects.

^{99m}Tc-sestamibi is a Food and Drug Administration–approved myocardial perfusion imaging agent that is indicated for detecting coronary artery disease in adults by localizing myocardial ischemia (reversible defects) and infarction (nonreversible defects), for evaluating myocardial function, and for developing information for use in patient management decisions. ^{99m}Tc-sestamibi is widely used in children for a variety of indications, ranging from the assessment of cardiac complications in Kawasaki disease to the management of transplant patients and patients with congenital defects of the heart, coronary circulation, and great vessels.

In common with all nuclear medicine procedures, studies using ^{99m}Tc-sestamibi result in a modest radiation dose to the patient. Although several studies have been conducted to assess the radiation dose due to ^{99m}Tc-sestamibi in adults (*4*), and these results have been mathematically extrapolated to children (*5,17*), no studies have been conducted in children to determine the best estimate of radiation dose. Mathematic extrapolation can account for differences in organ size and position between adults and children, but it assumes that the biologic distribution of the radiopharmaceutical is the same in both. This is a significant potential source of differences in the organ-by-organ radiation dose estimates. Accurate, age-dependent radiation dose data are an important component in deciding the frequency of use and administered dose of ^{99m}Tc-sestamibi in children and adolescents. In addition, no data currently exist documenting the safety and pharmacokinetic properties of ^{99m}Tc-sestamibi in this population.

TABLE 4
Overall Pharmacokinetic Values and Mean Urinary Excretion Fraction for PE Group

	Pharmacokinetic values				Urinary excretion fraction		
Analysis group	AUC(0-T) (%ID·h)	AUC(INF) (%ID·h)	Terminal T1/2	MRT	0–2 h	2–8 h	Total excretion
Rest							
Children (n = 13)	5.21 ± 1.81	6.86 ± 2.85	3.50 ± 1.20	3.73 ± 1.35	13.1 ± 5.0	4.8 ± 3.04	13.9 ± 6.63
Adolescents (n = 14)	4.04 ± 1.37	5.13 ± 1.65	3.13 ± 0.84	3.51 ± 1.12	15.0 ± 8.35	6.8 ± 5.14	17.2 ± 11.73
Stress							
Children (n = 10)	6.11 ± 1.97	8.20 ± 3.07	4.13 ± 1.19	4.22 ± 1.32	12.6 ± 5.15	6.5 ± 2.96	13.4 ± 6.54
Adolescents (n = 9)	5.43 ± 1.32	6.66 ± 1.82	3.10 ± 1.17	2.96 ± 1.19	10.1 ± 3.72	3.3 ± 1.62	8.4 ± 5.30
Overall (n = 46)	5.09 ± 1.76	6.59 ± 2.59	3.45 ± 1.13	3.62 ± 1.27	13.2 ± 6.09	5.4 ± 3.77	13.8 ± 8.59

AUC data units are mean ± SD time (h); urinary excretion units are expressed in %ID.

TABLE 5
Tabulation of Adverse Events

Primary system/organ	Children (n = 39)	Adolescents (n = 39)	Total (n = 78)
Any AE	11	4	15
General disorders and administration site reactions	4	1	5
Infusion site reaction	2	0	2
Chest pain	0	1	1
Fatigue	0	1	1
Infusion site pain	1	0	1
Pyrexia	1	0	1
Gastrointestinal disorders	3	0	3
Diarrhea	2	0	2
Flatulence	1	0	1
Nausea	1	0	1
Skin and subcutaneous disorders	3	0	3
Hyperhidrosis	1	0	1
Pruritis	1	0	1
Skin irritation	1	0	1
Nervous system disorders	0	2	2
Dizziness	0	1	1
Headache	0	1	1
Cardiac disorders	0	1	1
Atrioventricular block first degree	0	1	1
Eye disorders	1	0	1
Scleral hyperemia	1	0	1
Musculoskeletal and connective tissue disorders	1	0	1
Pain in the extremities	1	0	1
Respiratory, thoracic, and mediastinal disorders	0	1	1
Asthma exercise induced	0	1	1

In adults (*4*), the ULI wall was the critical organ, receiving 4.66 and 4.77 rad for stress and rest studies, respectively, after a 1,110-MBq (30-mCi) dose and assuming a 2-h voiding interval, equivalent to 0.155 and 0.159 rem/mCi (0.042 and 0.043 mSv/MBq), respectively. Subsequent recalculation, as documented in ICRP 80, reduced the values in the ULI to 0.027 mSv/MBq at rest and 0.022 mSv/MBq with stress (*17*). This recalculation also resulted in the identification of the gallbladder wall as the critical organ (0.036 mSv/MBq rest, 0.033 mSv/MBq stress). Blood pharmacokinetic information on ^{99m}Tc-sestamibi was reported in adult subjects during rest and post-exercise (*4*). This study also demonstrated that the decay-corrected blood clearance approximated a dual exponential curve with an initial fast component, with highly variable 36 ± 18 %ID peak activity at 1 min, 9 ± 0.6 %ID at 5 min, and a later slow component, falling to less than 1% within 1–2 h after injection. Data from the ^{99m}Tc-sestamibi package insert indicate that the hepatobiliary system provides the major pathway for clearance of ^{99m}Tc-sestamibi in adults, with 27 %ID excreted in urine.

In this study, the largest mean estimated organ-absorbed dose among all 47 DE subjects was to the ULI wall at 0.082 mSv/MBq (0.03 rem/mCi). The next largest absorbed organ doses in decreasing order were to the SI wall at 0.043 mSv/MBq (0.16 rem/mCi), to the gallbladder wall at 0.042 mSv/MBq (0.16 rem/mCi), and to the lower large intestine wall at 0.035 mSv/MBq (0.13 rem/mCi). The average EDE for ^{99m}Tc-sestamibi was 0.019 mSv/MBq (0.072 rem/mCi). The average ED for ^{99m}Tc-sestamibi was 0.015 mSv/MBq (0.055 rem/mCi).

It was possible to compare the injected dose per kg of body mass yielding 50 mSv to the critical organ derived from this study with clinical practice. For rest adolescents, using the body mass for the 15-y-old phantom, the result was 12 MBq/kg (0.31 mCi/kg).

For rest children, using the average of the body mass from the 5-y- and 10-y-old phantoms, the value was 16.9 MBq/kg (0.46 mCi/kg). The equivalent value for adults using the data from ICRP publication 80 (*17*) was 18.2 MBq/kg (0.50 mCi/kg). From the ^{99m}Tc-sestamibi package insert, this value was 14.7 MBq/kg (0.40 mCi/kg). The practice guideline for myocardial perfusion imaging in adults from the Society of Nuclear Medicine and Molecular Imaging suggests a dose of 1,110 MBq (30 mCi) per injection. Assuming a 70-kg patient, this yields 16 MBq/kg (0.43 mCi/kg). The values seen in both adolescents and children were similar in this study to both the guideline limiting dose and the current clinical practice for adults. The observation that the calculated limiting injected dose for adolescents was smaller than that for both children and adults raised the likelihood that the difference was more the result of variations in population and methodology than an observable change in the data. This suggests that the calculation of administered dose in pediatric subjects using body mass normalization based on the adult value

appears to be an appropriate practice, but pediatric doses should remain in the low end of recommended ranges.

In addition, the results of this study are comparable to the extrapolated values calculated using adult biodistribution data and phantoms representing children and adolescents. The value for adolescents in this study at rest (0.013 mSv/MBq) and stress (0.0099 mSv/MBq) is similar to the extrapolated value for the 15 y old (0.012 and 0.01 mSv/MBq for rest and stress, respectively). Similarly, the estimates for children at rest (0.02 mSv/MBq) and stress (0.017 mSv/MBq) fall between the extrapolated values for the 5 and 10 y olds (0.028 and 0.018 mSv/MBq) at rest and stress (0.016 and 0.023 mSv/MBq), suggesting that the primary contributor to the increased radiation dose to adolescents and children for ^{99m}Tc-sestamibi is the physical difference among the dosimetry models.

The blood %ID in WBBV was characterized by a rapid decline to 5 min after ^{99m}Tc-sestamibi administration, followed by a slower decline in the subsequent time points up to 6 h in the PE population. A similar trend was observed in the subset of 18 subjects in the DE + PE population. A significant difference was observed in %ID in WBBV over time between rest and stress subjects ($P = 0.0013$). The urinary excretion data were obtained from a nominal 8-h period, instead of a 24-h collection, because of difficulty in keeping the subjects and their families at the study site.

^{99m}Tc-sestamibi was well tolerated in this pediatric study population. The overall incidence of AEs was 19%, and the incidence was higher in children (28%) than in adolescents (10%). The only AEs experienced by at least 2 subjects in any group were diarrhea and infusion site reaction (2 subjects [3%] each). No deaths were reported. One child experienced an SAE (asthma) and 1 child discontinued due to an AE (infusion site reaction). Both events were considered unlikely related to the study drug by the investigators.

CONCLUSION

In this correspondence we presented the result of a phase I–II study for ^{99m}Tc-sestamibi in a pediatric population. Estimates of radiation dosimetry for ^{99m}Tc-sestamibi were similar to published extrapolations for children derived from studies in adults; therefore, current dosing regimens are appropriate. The pharmacokinetic parameters, AUC, T1/2, and MRT, were estimated in this pediatric population. The pharmacokinetic profile of %ID in blood in the study was also similar to the relevant published adult information.

DISCLOSURE

The costs of publication of this article were defrayed in part by the payment of page charges. Therefore, and solely to indicate this fact, this article is hereby marked "advertisement" in accordance with 18 USC section 1734. No potential conflict of interest relevant to this article was reported.

ACKNOWLEDGMENTS

On behalf of the coinvestigators (in alphabetical order) of the ^{99m}Tc-sestamibi®-201 study and the related institutions: Joseph Cava, MD, Children's Hospital of Wisconsin, Milwaukee, WI, USA; Nagib Dahdah, MD, CHU Sainte-Justine, Montreal, Qc, Canada; Ziyad Hijazi, MD, University of Chicago Children's Hospital, Chicago, IL, USA; Beth Kaufman, MD, Children's Hospital of Philadelphia, Philadelphia, PA, USA; Meng-Luen Lee, MD, Changhua Christian Hospital, Changhua, Taiwan; Wan-Yu Lin, MD, Veteran's General Hospital, Tai Chung, Taiwan; Marian Melish, MD, Kapiolani Medical Center for Women and Children, Honolulu, HI, USA; Helen Nadel, MD, British Columbia's Children's Hospital, Vancouver, BC, Canada; Michael Portman, MD, Children's Hospital and Regional Medical Center, Seattle, WA, USA; Mei-Huan Wu, MD, National Taiwan University Hospital, Taipei, Taiwan. This study was registered under www.clinicaltrials.govidentifier number NCT00162045.

REFERENCES

1. Robinson B, Goudie B, Remmert J, Gidding SS. Usefulness of myocardial perfusion imaging with exercise testing in children. *Pediatr Cardiol.* 2012;33:1061–1068.
2. Kondo C. Myocardial perfusion imaging in pediatric cardiology. *Ann Nucl Med.* 2004;18:551–561.
3. Velasco-Sanchez D, Lambert R, Turpin S, et al. Right ventricle myocardial perfusion scintigraphy: feasibility and expected values in children. *Pediatr Cardiol.* 2012;33:295–301.
4. Wackers FJ, Berman DS, Maddahi J, et al. Technetium-99m hexakis 2-methoxyisobutyl isonitrile: human biodistribution, dosimetry, safety, and preliminary comparison to thallium-201 for myocardial perfusion imaging. *J Nucl Med.* 1989;30:301–311.
5. Stabin M, Gelfand M. Dosimetry of pediatric nuclear medicine procedures. *Q J Nucl Med.* 1998;42:93–112.
6. International Commission on Radiological Protection (ICRP). Radiation dose to patients from radiopharmaceuticals: addendum 2 to ICRP publication 53. ICRP publication 80. *Ann ICRP.* 1998;28:110–111.
7. Cardiolite Prescribing Information [package insert]. North Billerica, MA: Lantheus Medical Imaging; 2010.
8. Schillaci O, Banci M, Scopinaro F, et al. Myocardial scintigraphy with ^{99m}Tc-sestamibi in children with Kawasaki disease. *Angiology.* 1995;46:1009–1014.
9. Gadd R, Mountford PJ, Oxtoby JW. Effective dose to children and adolescents from radiopharmaceuticals. *Nucl Med Commun.* 1999;20:569–573.
10. Weindling SN, Wernovsky G, Colan SD, et al. Myocardial perfusion, function and exercise tolerance after the arterial switch operation. *J Am Coll Cardiol.* 1994;23:424–433.
11. Siegel JA, Thomas SR, Stubbs JB, et al. MIRD pamphlet no. 16: techniques for quantitative radiopharmaceutical biodistribution data acquisition and analysis for use in human radiation dose estimates. *J Nucl Med.* 1999;40:37S–61S.
12. Cristy M, Eckerman K. *Specific Absorbed Fractions of Energy at Various Ages from Internal Photon Sources*. ORNL/TM-8381/V1-V7. Oak Ridge, TN: Oak Ridge National Laboratory; 1987.
13. International Commission on Radiological Protection (ICRP). International Commission on Radiological Protection publication 26: recommendations of the International Commission on Radiological Protection. *Ann ICRP.* 1977;1.
14. International Commission on Radiological Protection (ICRP). International Commission on Radiological Protection publication 60: 1990 recommendations of the International Commission on Radiological Protection. *Ann ICRP.* 1991;21.
15. Newburger JW, Takahashi M, Gerber MA, et al. Diagnosis, treatment, and long-term management of Kawasaki disease: a statement for health professionals from the Committee on Rheumatic Fever, Endocarditis, and Kawasaki Disease, Council on Cardiovascular Disease in the Young, American Heart Association. *Pediatrics.* 2004;114:1708–1733.
16. Lipshultz SE, Sleeper LA, Towbin JA, et al. The incidence of pediatric cardiomyopathy in two regions of the United States. *N Engl J Med.* 2003;348:1647–1655.
17. International Commission on Radiological Protection (ICRP). International Commission on Radiological Protection publication 80: 1998. Radiation dose to patients from radiopharmaceuticals, addendum 2 to ICRP publication 53. *Ann ICRP.* 1998;28:107.